

Supporting Information

Mechanism Elucidation of the *cis-trans* Isomerization of an Azole Ruthenium-Nitrosyl complex and its Osmium Counterpart

Anatolie Gavriluta,^{a,b} Gabriel E. Büchel,^{a,b} Leon Freitag,^c Ghenadie Novitchi^{*,a,d}
Jean Bernard Tommasino,^a Erwann Jeanneau,^a Paul-Steffen Kuhn,^b
Leticia González,^{*c} Vladimir B. Arion^{*,b} and Dominique Luneau^{*,a}

^a *Université Claude Bernard Lyon 1, Laboratoire des Multimatériaux et Interfaces (UMR 5615), Campus de la Doua, 69622 Villeurbanne Cedex, France*

^b *University of Vienna, Institute of Inorganic Chemistry, Währinger Strasse 42, A-1090 Vienna, Austria*

^c *University of Vienna, Institute of Theoretical Chemistry, Währinger Strasse 17, A-1090 Vienna, Austria*

^d *Laboratoire National des Champs Magnétiques Intenses-CNRS, Université Joseph Fourier, 25 Avenue des Martyrs, 38042 Grenoble Cedex 9, France*

Ruthenium-, osmium-nitrosyl, 1*H*-indazole, *cis-trans* isomerization

Corresponding Authors :

*E-mail: ghenadie.novitchi@lnmi.cnrs.fr, (G. N.); leticia.gonzalez@univie.ac.at (L.G.)
vladimir.arion@univie.ac.at (V. B. A.); luneau@univ-lyon1.fr (D. L.);

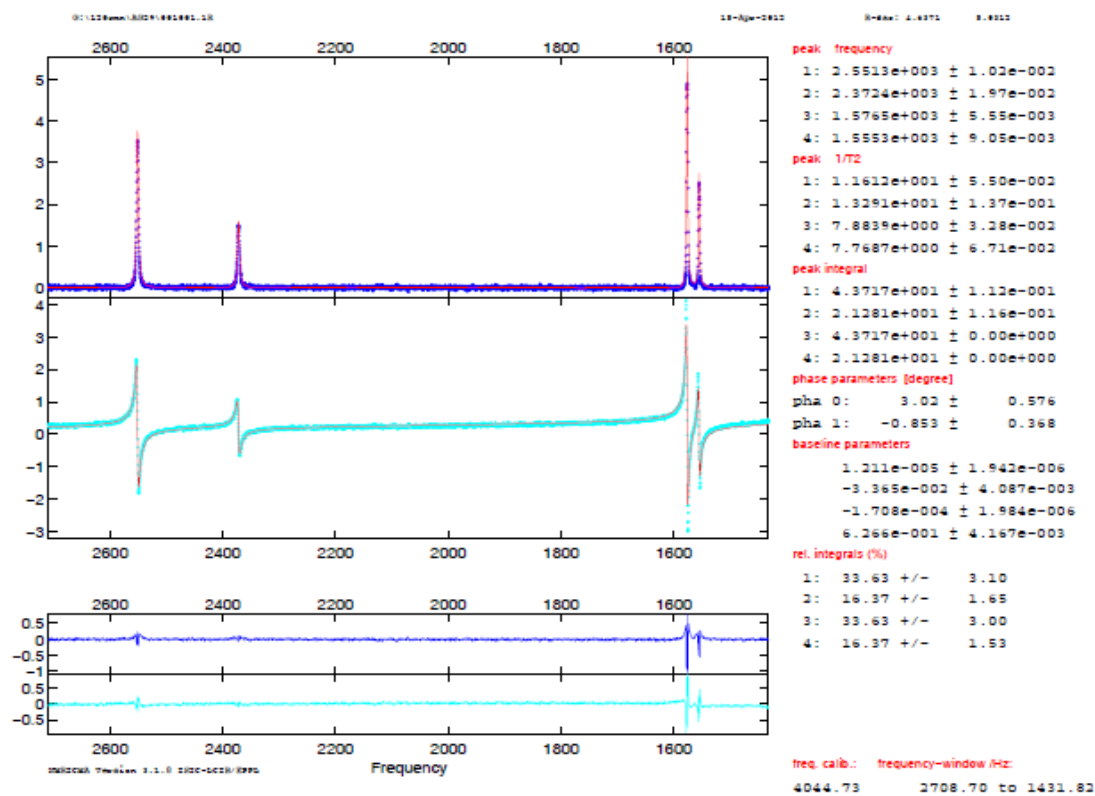


Figure S1 Simultaneous fitting of the real (top) and imaginary (bottom) part of an ^1H NMR spectrum using *NMRICMA* program (Helm, L. *NMRICMA*, 3.1.5; EPFL: Lausanne, 2003.)

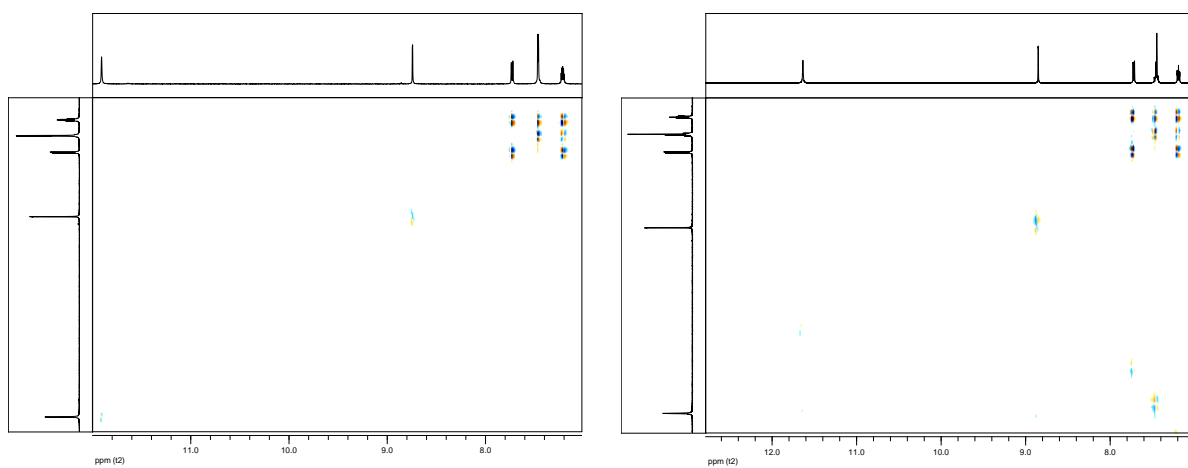


Figure S2 ^1H , ^1H COSY NMR spectra (500 MHz) of *cis* (left) and *trans* (right) $[\text{RuCl}_4(\text{NO})(\text{indz})]^-$ in $\text{C}_2\text{D}_2\text{Cl}_4$ solution. The blue stars correspond to residual isomer present in solution

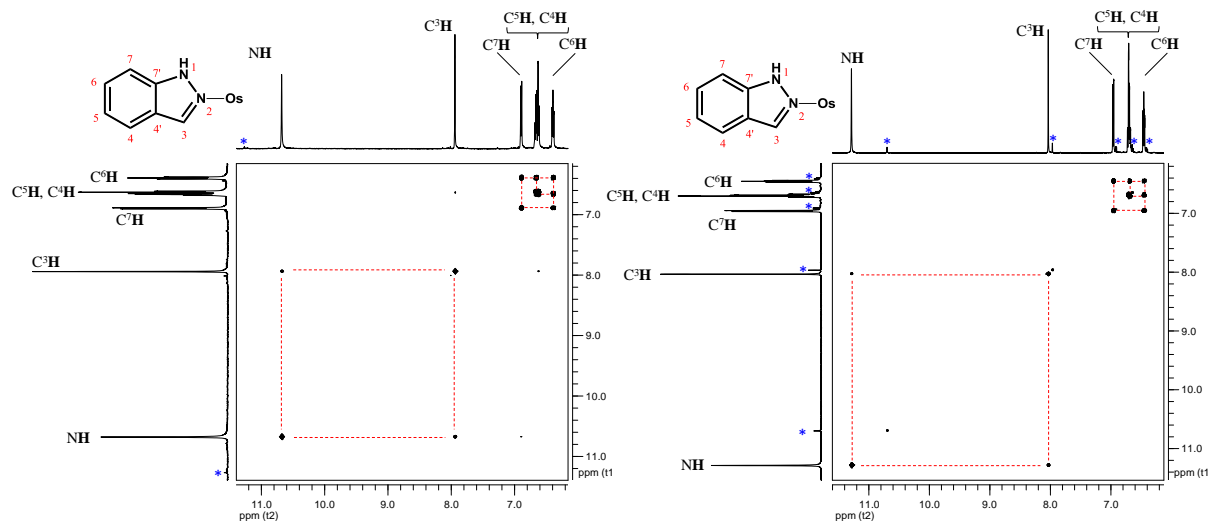


Figure S3 $^1\text{H}, ^1\text{H}$ COSY NMR spectra (500 MHz) of *trans* (left) and *cis* (right) $[\text{OsCl}_4(\text{NO})(\text{indz})]^-$ in $\text{C}_2\text{D}_2\text{Cl}_4$ solution. The blues stars correspond to residual isomer presenting solution.

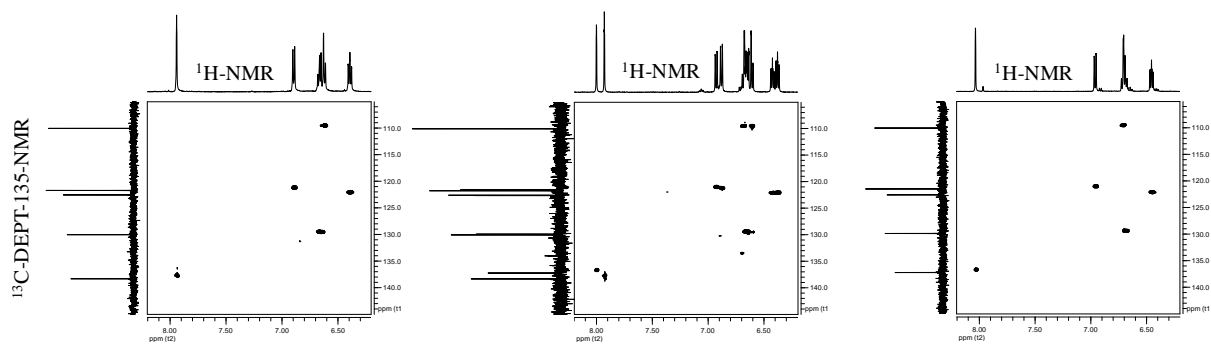


Figure S4 $^1\text{H}, ^{13}\text{C}$ HSQC NMR spectra of *trans* (left), *cis* (right) $[\text{OsCl}_4(\text{NO})(\text{indz})]^-$ and mixture of *trans* and *cis* (in middle) during the isomerization transformation

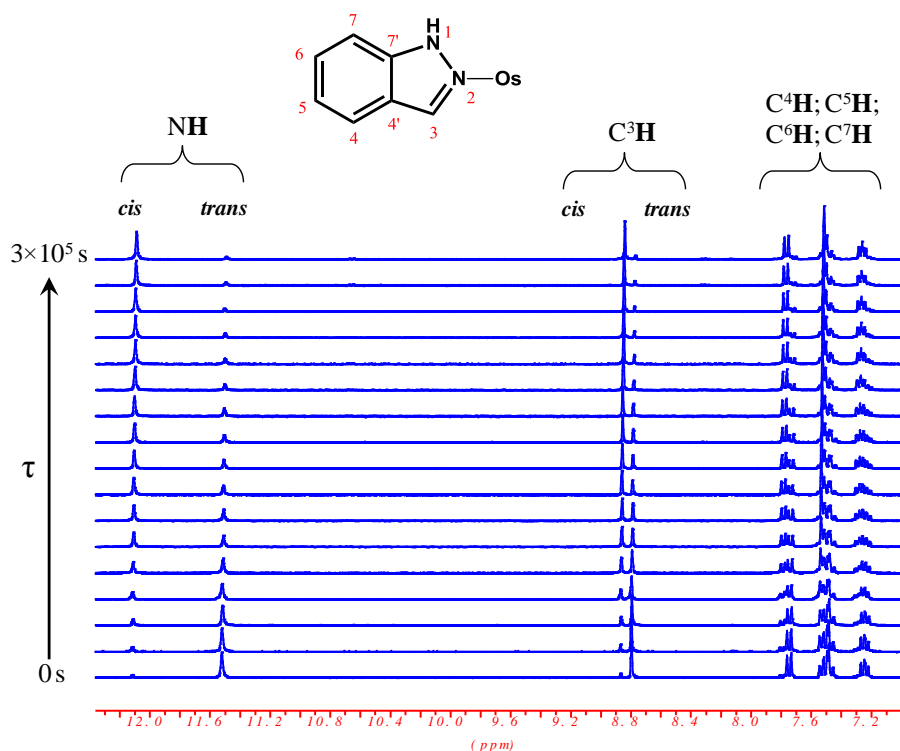


Figure S5 Evolution of ^1H NMR spectra (300MHz) of $\text{trans-}[\text{OsCl}_4(\text{NO})(\text{Ind})]^-$ isomer function of time ($\tau=0\div 3\times 10^5\text{s}$) after heating at 120°C in $\text{C}_2\text{D}_2\text{Cl}_4$ solution ($C_{\text{cis+trans}}=15.26\text{ mmol/L}$) showing the formation of the *cis* isomer. (Aromatic region).

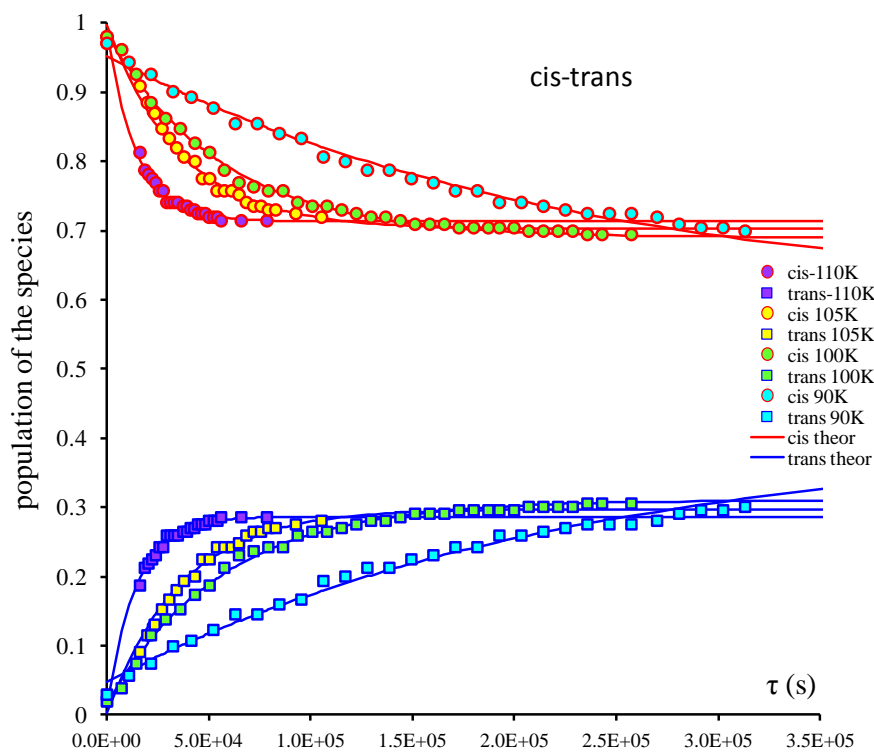


Figure S6. NMR Kinetics of the *cis* to *trans* isomerization for $[\text{RuCl}_4(\text{NO})(\text{Hind})]^-$. The solid line corresponds to best fit according reversible 1-st order process at indicated temperatures.

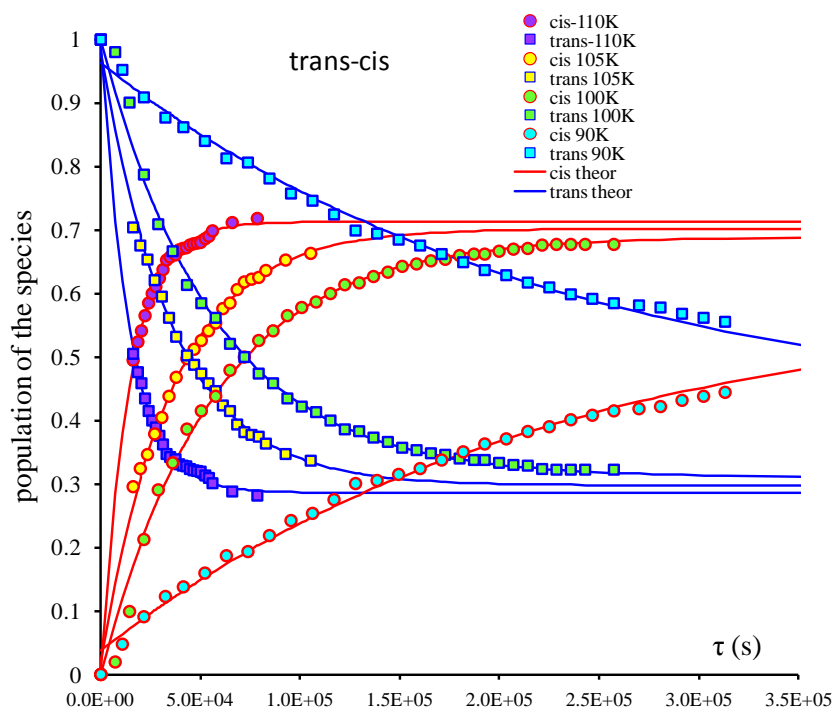


Figure S7. NMR Kinetics of the *trans* to *cis* isomerization for $[\text{RuCl}_4(\text{NO})(\text{Hind})]$. The solid line corresponds to best fit according reversible I-st order process at indicated temperatures.

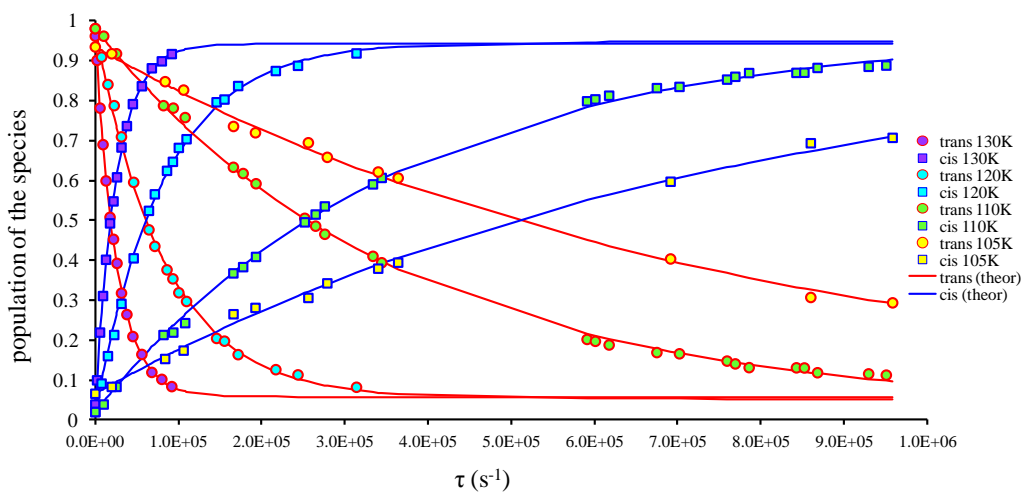


Figure S8. NMR Kinetics of the *trans/cis* isomerization for $[\text{OsCl}_4(\text{NO})(\text{indz})]$. The solid line corresponds to best fit according reversible I-st order process at indicated temperatures.

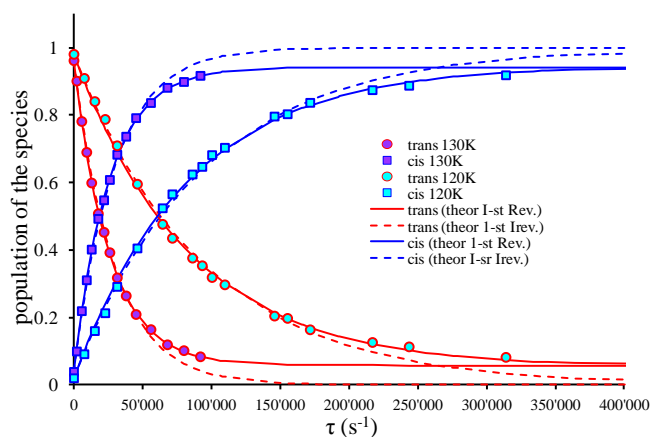


Figure S9. NMR Kinetics of the *trans-cis* isomerization for $[\text{OsCl}_4(\text{NO})(\text{indz})]^-$. The solid line correspond to best fit according reversible I-st order and the dashed line correspond to irreversible I-st order reaction at indicated temperatures.

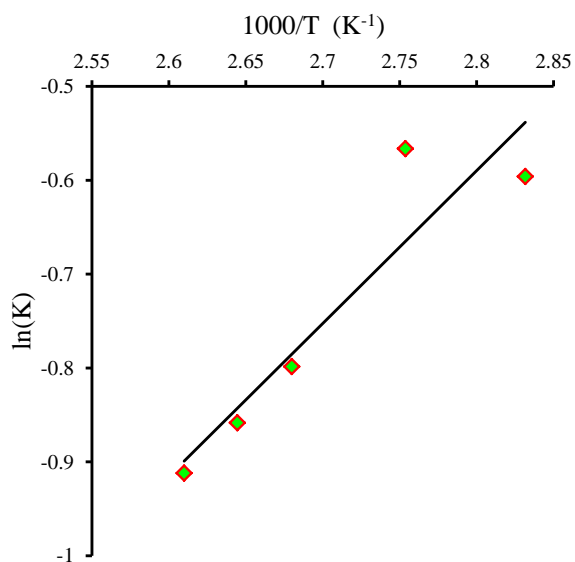


Figure S10 van't Hoff plot for *cis/trans* isomerization of $[\text{RuCl}_4(\text{NO})(\text{Hind})]^-$. Solid line correspond to best fit with following thermodynamic parameters $\Delta H^\circ = 13.5 \pm 1.5$ kJ/mol $\Delta S^\circ = -5.2 \pm 3.4$ J/(mol·K)

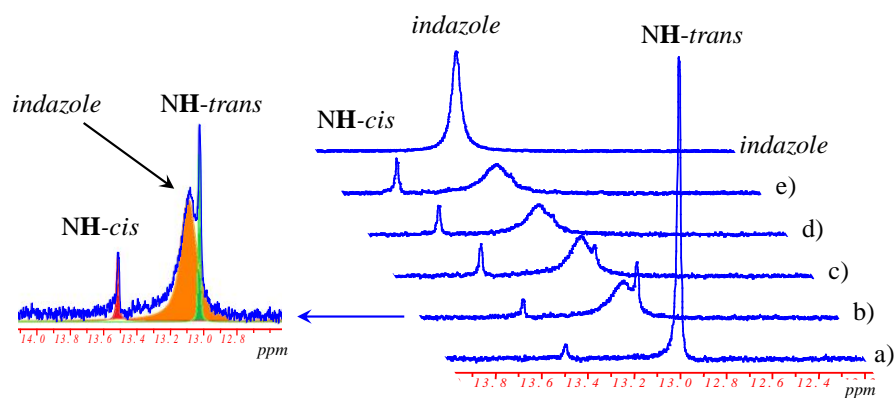


Figure S11. Evolution of ^1H NMR spectra (300MHz) of $\text{trans-}[\text{OsCl}_4(\text{NO})(\text{Ind})]^-$ isomer function of time: b) 2 days; c) 3 days; d) 4 days; e) 5 days after heating at 100°C in DMSO solution ($C_{\text{cis+trans}}=18.51 \text{ mmol/L}$). In the left is deconvolution and assignments of signals.

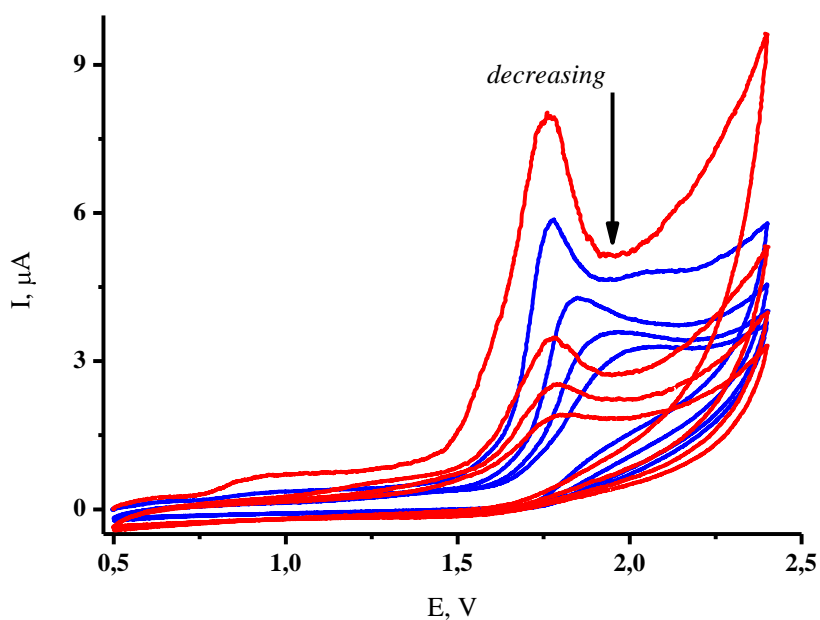


Figure S12. Oxidation of $\text{cis-}[\text{RuCl}_4(\text{NO})(\text{Hind})]^-$, (red) and $\text{trans-}[\text{RuCl}_4(\text{NO})(\text{Hind})]^-$, (blue) by cyclic voltammetry in the same experimental condition as Os isomers

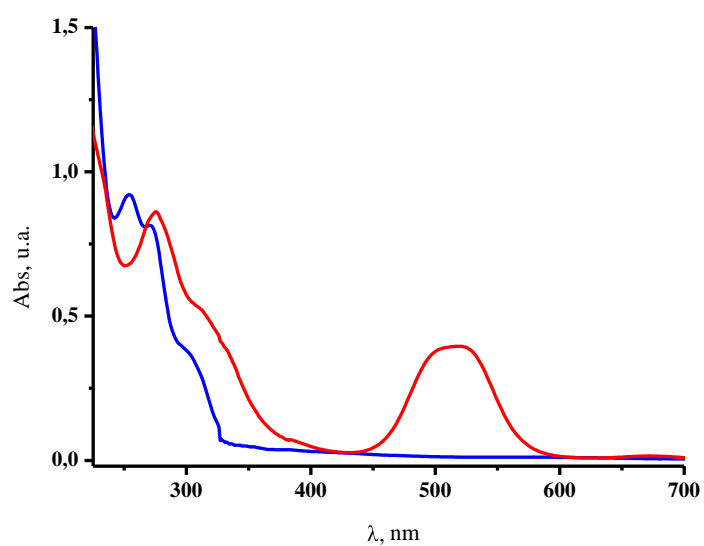


Figure S13. UV-vis spectra of acetoneitrile solutions (0.1M) of *trans*-[OsCl₄(NO)(Hind)]⁻, before (blue) and after (red) electrolysis.

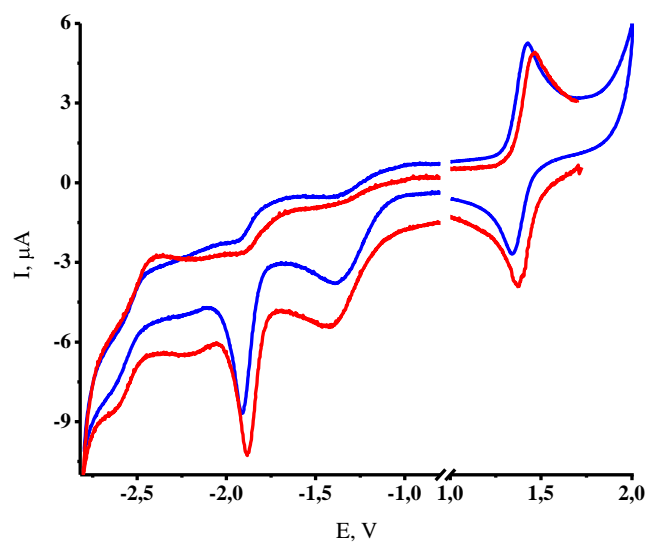


Figure S14. Cyclic voltammetry of *trans*-[OsCl₄(NO)(Hind)]⁻, before (blue) and after (red) electrolysis.

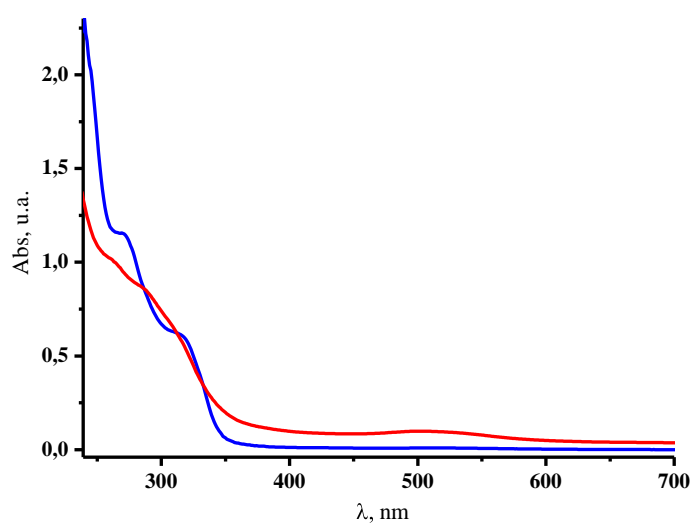


Figure S15. UV-vis spectra of acetonitrile solutions (0.1M) of *cis*-[OsCl₄(NO)(Hind)]⁻, before (blue) and after (red) electrolysis.

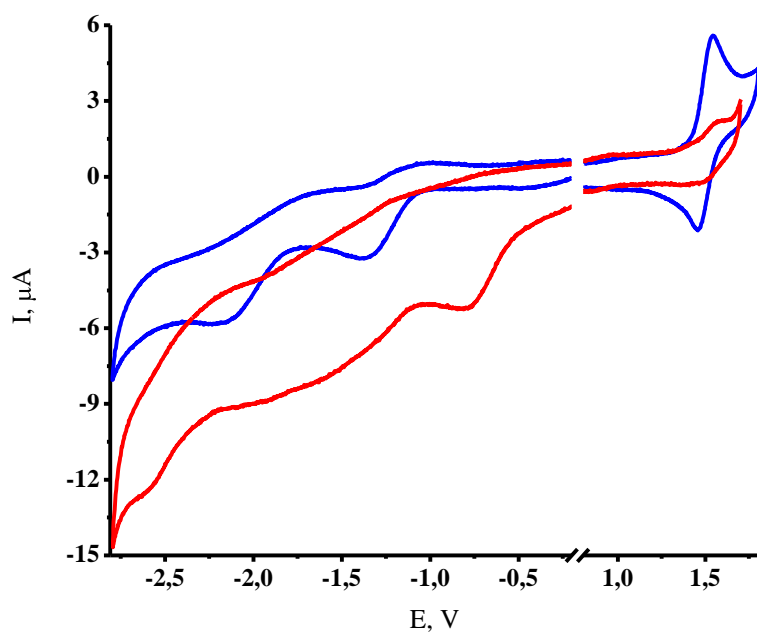


Figure S16. Cyclic voltammetry of *cis*-[OsCl₄(NO)(Hind)]⁻, before (blue) and after (red) electrolysis.

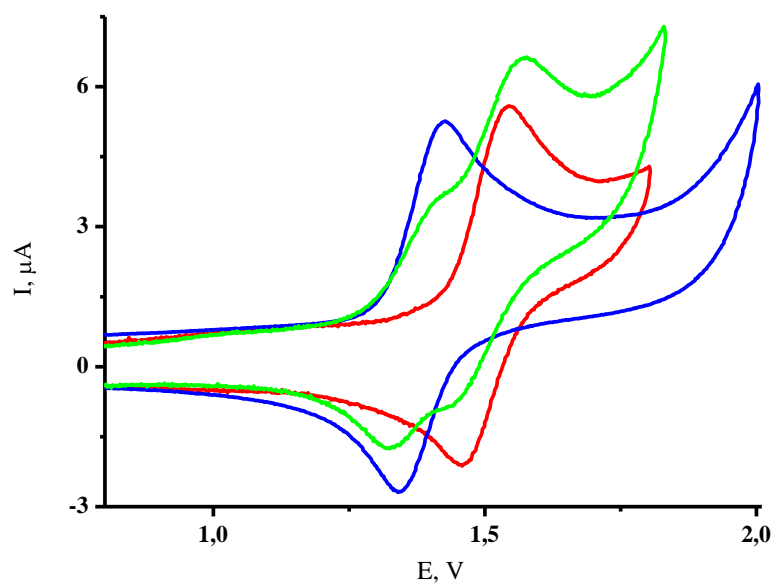


Figure S17. Cyclic voltammetry of *cis*-[OsCl₄(NO)(Hind)]⁻, (red), *trans*-[OsCl₄(NO)(Hind)]⁻, (blue) and their mixture (green) at 100 mV/s on GC electrode (3 mm) in acetonitril solution.

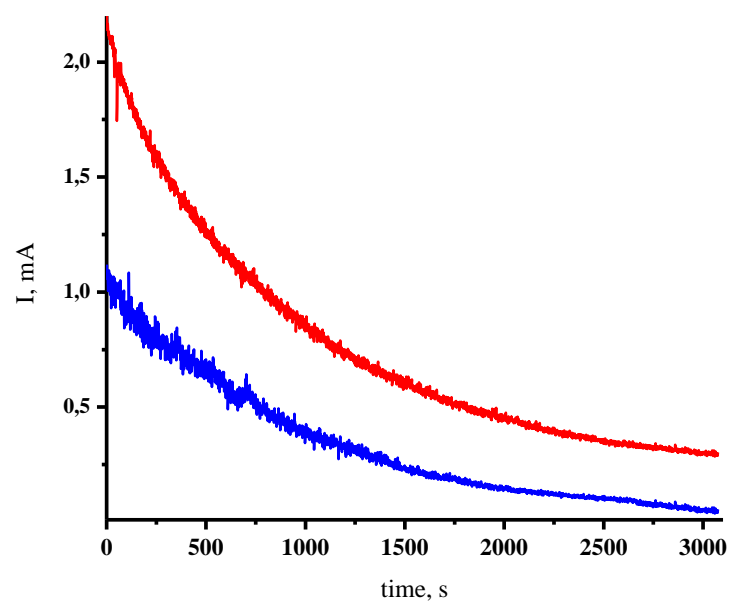


Figure S18. Exhaustive electrolysis of *cis*-[OsCl₄(NO)(Hind)]⁻, (red) – corresponding 2e and *trans*-[OsCl₄(NO)(Hind)]⁻, (blue) – corresponding 1e.

All geometries reported below have been optimized at the B3LYP/6-31G* level of theory.

Optimised structures of 1 and 2:

Table S1. Optimised structure of *cis*-[RuCl₄(NO)(Hind)]⁻

Ru	-1.276071	0.011832	0.061736
Cl	-1.036380	-2.426595	0.090517
Cl	-1.049035	-0.096205	-2.300444
Cl	-1.461495	2.416166	-0.141124
Cl	-3.654993	-0.203862	-0.205199
O	-1.498289	0.115384	2.963741
N	0.835484	0.178292	0.078594
N	1.598765	-0.939217	0.031052
H	1.090125	-1.844591	0.012385
N	-1.409839	0.077743	1.804046
C	1.637940	1.249245	0.107227
H	1.196301	2.252773	0.137315
C	2.996569	0.815010	0.079427
C	4.263281	1.455751	0.092531
H	4.338657	2.554243	0.131952
C	5.405131	0.655505	0.055214
H	6.401859	1.126316	0.064455
C	5.313271	-0.768110	0.005179
H	6.241631	-1.362305	-0.023018
C	4.083949	-1.429524	-0.008790
H	4.015358	-2.527323	-0.046786
C	2.926112	-0.618194	0.029130

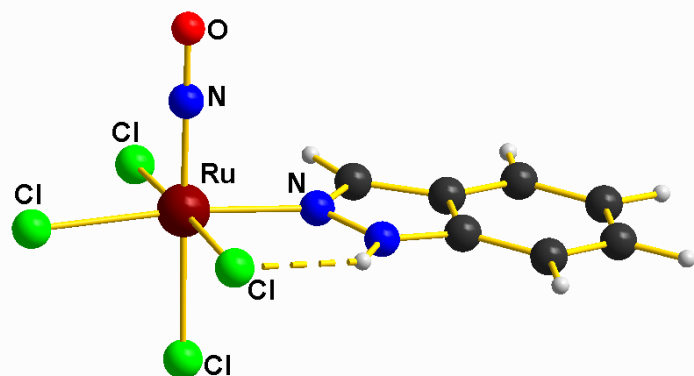
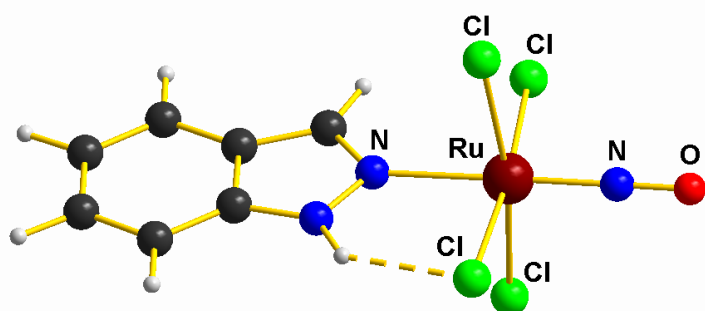
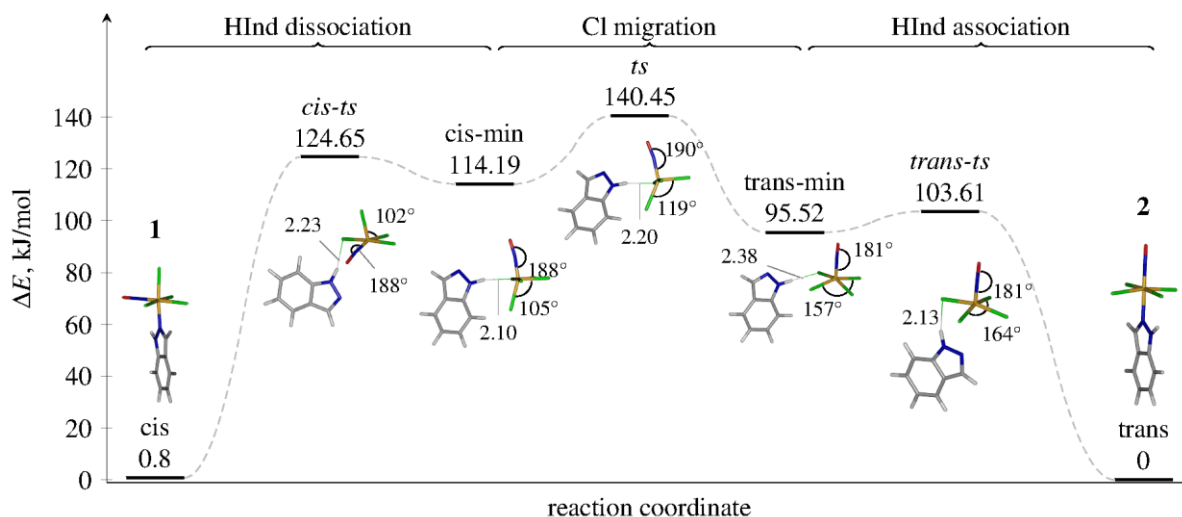


Table S2. Optimised structure of *trans*-[RuCl₄(NO)(Hind)]⁻

Ru	1.361441	0.005087	0.000132
Cl	1.434180	2.413687	0.000189
Cl	1.162027	0.016383	2.403711
Cl	1.043858	-2.416562	0.000109
Cl	1.163296	0.016491	-2.403625
N	-0.792805	0.165964	-0.000251
N	-1.561942	-0.946922	-0.000327
H	-1.059492	-1.854941	-0.000219
C	-1.594460	1.238496	-0.000162
H	-1.152240	2.241756	-0.000101
C	-2.954406	0.809996	-0.000163
C	-4.219069	1.455293	-0.000096
H	-4.290699	2.554792	-0.000046
C	-5.363232	0.657818	-0.000154
H	-6.358769	1.131247	-0.000142
C	-5.275555	-0.767304	-0.000272
H	-6.206016	-1.358879	-0.000325
C	-4.048499	-1.432866	-0.000298
H	-3.983381	-2.531564	-0.000279
C	-2.888354	-0.623710	-0.000263
N	3.091568	-0.147613	0.000181
O	4.247749	-0.261563	-0.000097





Transition states and intermediates for the dissociative mechanism

Table S3. Optimised structure of the *cis-ts* transition state (cf. Fig. 9a)

Ru	-1.8286261	-0.2630592	-0.0122971
Cl	-0.2068541	-2.0733541	0.3057911
Cl	-1.4937186	-0.5293395	-2.2925932
Cl	-3.2195174	1.6023672	-0.5326078
Cl	-3.5912617	-1.6884653	0.4694141
O	-1.2654225	0.7782187	2.6441964
N	1.8142508	1.3265149	0.2989244
N	2.1362990	0.0248128	0.1516627
H	1.3697516	-0.6953116	0.1505347
N	-1.5695977	0.3075682	1.6164919
C	2.9596347	2.0120584	0.2833604
H	2.9416899	3.1059534	0.3878927
C	4.0830113	1.1358408	0.1229000
C	5.4913736	1.2608549	0.0368175
H	5.9730217	2.2519478	0.0958641
C	6.2587015	0.1047703	-0.1295604
H	7.3571454	0.1828196	-0.2002593
C	5.6480637	-1.1799515	-0.2089641
H	6.2862615	-2.0702583	-0.3427308
C	4.2622404	-1.3380454	-0.1279116
H	3.7856815	-2.3289793	-0.1939191
C	3.4868779	-0.1679454	0.0407627

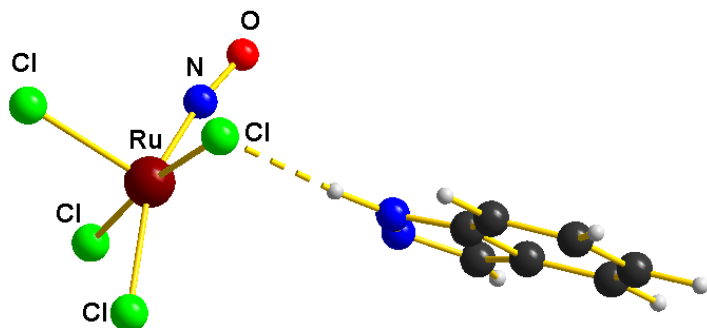


Table S4. Optimised structure of the *cis-min* intermediate (cf. Fig. 9a)

Ru	-2.144979	-0.836111	-0.381036
Cl	-0.764606	-1.413157	1.526221
Cl	-0.503320	-1.819543	-1.716319
Cl	-3.259121	-0.202294	-2.402443
Cl	-3.555493	-2.628719	0.026116
O	-3.509202	1.221653	1.151385
N	2.140927	1.411474	2.106682
N	1.929373	0.400074	1.228593
H	1.035046	-0.128384	1.257405
N	-3.034452	0.341181	0.559133
C	3.387223	1.844478	1.893741
H	3.789971	2.675765	2.490197
C	4.026389	1.094116	0.851360
C	5.294753	1.087459	0.216237
H	6.078597	1.803428	0.513945
C	5.526393	0.149813	-0.794183
H	6.505059	0.123614	-1.301660
C	4.517881	-0.778929	-1.187569
H	4.738548	-1.500535	-1.991937
C	3.258058	-0.796841	-0.581352
H	2.473596	-1.505641	-0.889451
C	3.027678	0.149435	0.444079

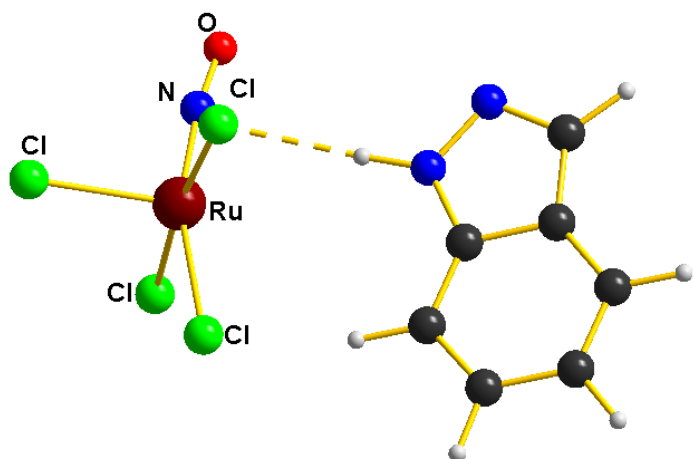


Table S5. Optimised structure of the *ts* transition state (cf. Fig. 9a)

Ru	-1.8193053	-0.0106152	-0.0338891
Cl	-0.2859209	-1.3440147	1.3035224
Cl	-0.5407613	-0.6172464	-1.8890175
Cl	-3.2099955	1.2016667	-1.5494331
Cl	-3.5753555	-1.3903300	0.5912617
O	-1.9737374	2.0822640	1.9559744
N	3.3291395	0.4373665	2.3112381
N	2.6867923	-0.0679774	1.2348418
H	1.6925896	-0.3823435	1.3076510
N	-1.9947709	1.1812292	1.2046979
C	4.5805789	0.6920984	1.9193964
H	5.2984683	1.1189110	2.6347203
C	4.7800417	0.3402200	0.5439752
C	5.8436480	0.3720296	-0.3923081
H	6.8379216	0.7540974	-0.1039023
C	5.6044836	-0.0890099	-1.6891517
H	6.4187970	-0.0722776	-2.4338062
C	4.3229588	-0.5795563	-2.0744192
H	4.1714098	-0.9283859	-3.1101260
C	3.2518316	-0.6222777	-1.1786122
H	2.2514629	-0.9806274	-1.4699580
C	3.4998699	-0.1601000	0.1338772

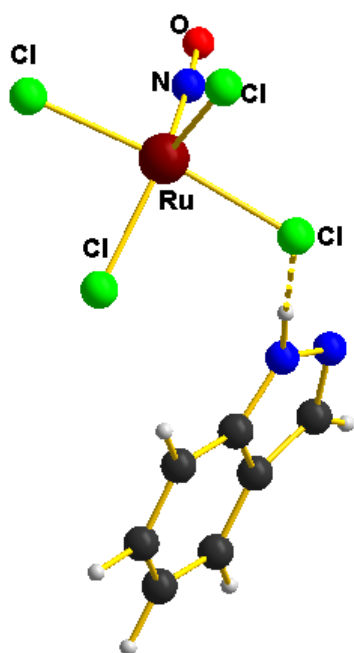


Table S6. Optimised structure of the *trans-min* intermediate (cf. Fig. 9a)

Ru	-2.300696	-0.935220	-0.144921
Cl	-0.995646	-0.729878	1.829660
Cl	-0.548650	0.178844	-1.283562
Cl	-3.017384	-1.788944	-2.225793
Cl	-3.433475	-2.729036	0.888526
O	-4.192845	1.192473	0.204549
N	2.337065	1.333990	2.221004
N	1.996747	0.585715	1.143899
H	1.017402	0.270347	1.035239
N	-3.417416	0.330971	0.068643
C	3.651791	1.555514	2.129420
H	4.163324	2.151935	2.898549
C	4.202213	0.931170	0.961219
C	5.483459	0.816547	0.363681
H	6.365044	1.292593	0.824198
C	5.600994	0.085068	-0.821374
H	6.587078	-0.018829	-1.303982
C	4.465799	-0.532878	-1.424082
H	4.598563	-1.099933	-2.360769
C	3.189908	-0.437537	-0.860338
H	2.311839	-0.907991	-1.329285
C	3.072916	0.300449	0.340999

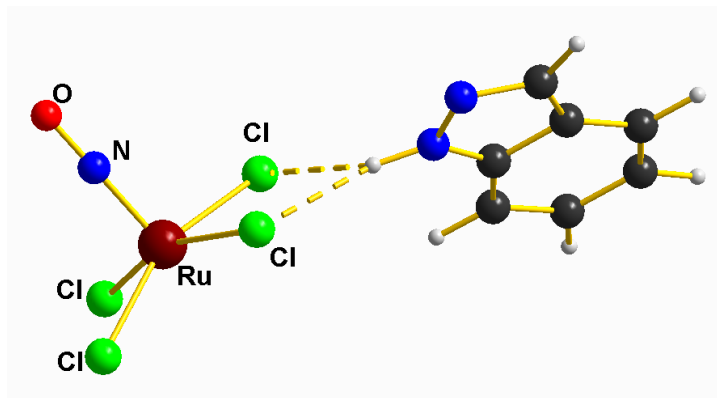
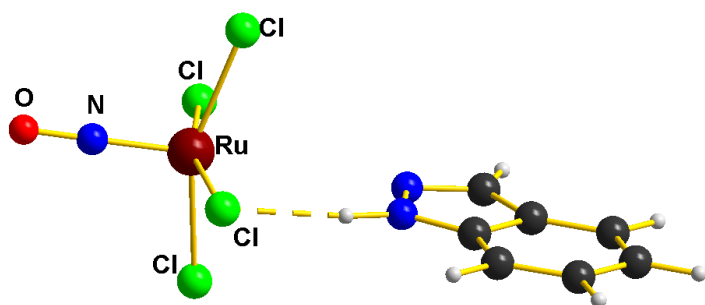
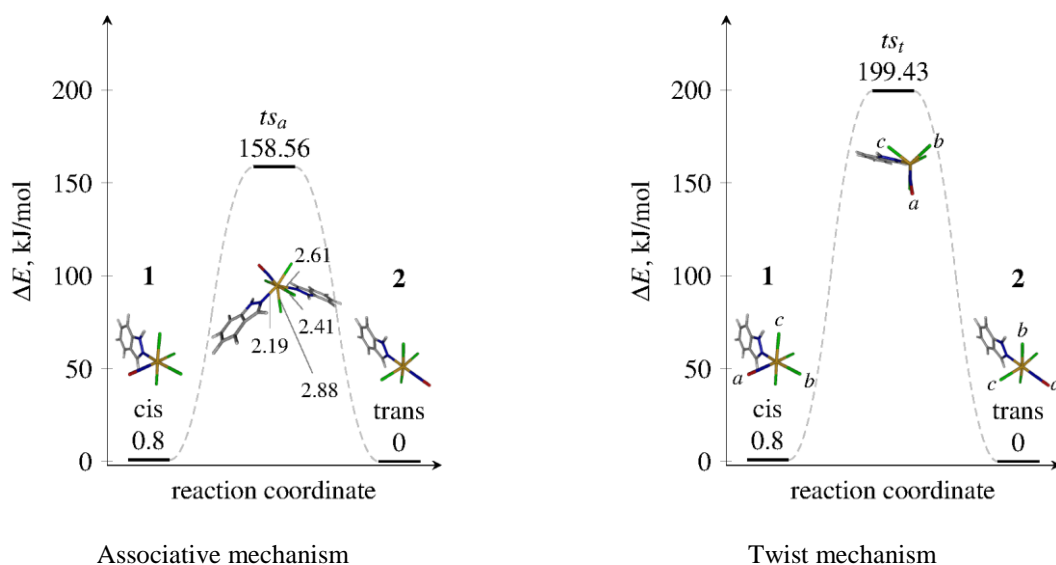


Table S7. Optimised structure of the *trans-ts* transition state (cf. Fig. 9a)

Ru	1.7052941	-0.0631116	-0.0492646
Cl	2.4122990	2.1801582	-0.1140155
Cl	1.4143159	0.1596188	2.2794955
Cl	0.3556797	-2.0700721	0.0516608
Cl	1.1288071	0.1077541	-2.3287113
N	-1.8014738	1.0767546	0.0740692
N	-2.1978278	-0.2109422	0.0695651
H	-1.4549794	-0.9472819	0.0674215
C	-2.9063875	1.8229956	0.0584086
H	-2.8234096	2.9185192	0.0587966
C	-4.0810403	1.0004191	0.0411430
C	-5.4830324	1.1990415	0.0189166
H	-5.9058759	2.2182114	0.0112030
C	-6.3204347	0.0800058	0.0058419
H	-7.4154352	0.2158518	-0.0122880
C	-5.7852304	-1.2398020	0.0148670
H	-6.4764512	-2.1000669	0.0041247
C	-4.4069742	-1.4705142	0.0362878
H	-3.9928725	-2.4914121	0.0427322
C	-3.5604535	-0.3386239	0.0488434
N	3.2157399	-0.8318155	-0.1338248
O	4.2795514	-1.3277369	-0.1926170





Transition states for the associative and twist mechanism

Table S8. Optimised structure of the transition state of the associative mechanism (cf. Fig. 9b)

Ru	0.040050	-0.076913	0.200593
N	0.321857	-0.198382	1.873079
O	0.414491	-0.274272	3.029111
Cl	-1.813033	0.246347	-1.989402
Cl	2.520750	-0.383226	0.174489
Cl	-0.295061	-2.452649	-0.090328
N	1.009905	-0.104535	-2.237677
C	1.577838	0.781650	-3.029880
C	1.899590	0.185969	-4.287177
C	1.461884	-1.163311	-4.161598
N	0.954807	-1.274464	-2.903160
C	2.494503	0.608139	-5.489824
C	2.632810	-0.306893	-6.523516
C	2.187559	-1.642739	-6.380327
C	1.600220	-2.091586	-5.206226
Cl	0.281496	2.328200	0.139716
N	-2.058765	0.157396	0.786315
N	-2.603129	1.391025	0.871285
C	-3.909301	1.312686	1.240929
C	-4.181830	-0.064737	1.467287
C	-2.961382	-0.731415	1.162579
C	-4.886145	2.305878	1.425631
C	-6.138135	1.885945	1.844749
C	-6.426783	0.519213	2.082626
C	-5.462995	-0.458307	1.898880
H	-2.053960	2.147633	0.466645
H	-2.709224	-1.781534	1.151932
H	-5.688246	-1.506242	2.077154
H	-7.424186	0.239194	2.410952
H	-6.922273	2.624061	1.993569
H	-4.668446	3.353656	1.242390
H	0.471739	-2.038337	-2.443857
H	1.259571	-3.117678	-5.099101
H	2.308952	-2.333384	-7.211720

H	1.726208	1.792168	-2.677380
H	3.088867	0.001829	-7.461097
H	2.837100	1.633480	-5.605949

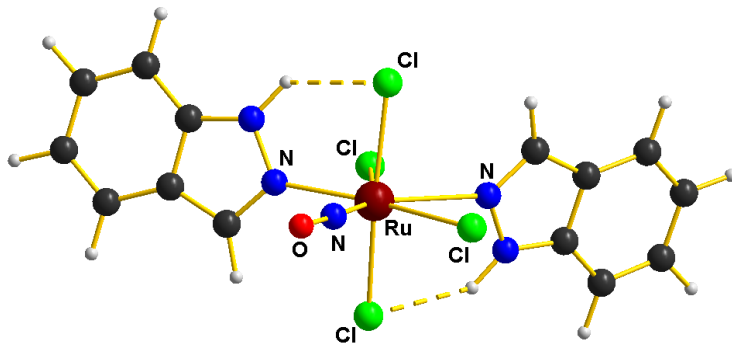


Table S9. Optimised structure of the transition state of the twist mechanism (cf. Fig. 9c)

Ru	-0.002133	-0.004186	-0.003193
N	-0.002965	0.002165	2.475156
C	-0.297303	-0.960282	3.330805
C	0.100306	-0.585947	4.647175
C	0.669792	0.709135	4.497157
N	0.590721	1.002004	3.171712
C	0.044159	-1.174436	5.925222
C	0.545622	-0.465097	7.004405
C	1.104635	0.826142	6.835024
C	1.177239	1.432392	5.591043
N	1.287736	-0.008314	-1.138860
O	2.090310	-0.182434	-1.960263
Cl	-1.933396	-1.346514	0.522179
Cl	-1.457592	0.844652	-1.721916
Cl	0.317297	2.341364	0.465335
Cl	1.391708	-2.140459	0.616705
H	0.811029	1.841244	2.642643
H	-0.761188	-1.863732	2.966073
H	-0.383407	-2.164690	6.057826
H	0.513266	-0.900459	7.999789
H	1.487708	1.353604	7.705314
H	1.608390	2.421508	5.465845

